



HAL
open science

Depth distribution of cesium-137 in paddy fields across the Fukushima pollution plume in 2013

Hugo Lepage, O. Evrard, Yuichi Onda, Irène Lefèvre, J. Patrick Laceby,
Sophie Ayrault

► **To cite this version:**

Hugo Lepage, O. Evrard, Yuichi Onda, Irène Lefèvre, J. Patrick Laceby, et al.. Depth distribution of cesium-137 in paddy fields across the Fukushima pollution plume in 2013. *Journal of Environmental Radioactivity*, 2015, 147, pp.157 - 164. 10.1016/j.jenvrad.2015.05.003 . hal-01806119

HAL Id: hal-01806119

<https://hal.science/hal-01806119>

Submitted on 14 May 2020

HAL is a multi-disciplinary open access archive for the deposit and dissemination of scientific research documents, whether they are published or not. The documents may come from teaching and research institutions in France or abroad, or from public or private research centers.

L'archive ouverte pluridisciplinaire **HAL**, est destinée au dépôt et à la diffusion de documents scientifiques de niveau recherche, publiés ou non, émanant des établissements d'enseignement et de recherche français ou étrangers, des laboratoires publics ou privés.

Depth distribution of cesium-137 in paddy fields across the Fukushima pollution plume in 2013

Hugo Lepage^{a,*}, Olivier Evrard^a, Yuichi Onda^b, Irène Lefèvre^a, J. Patrick Lacey^a, Sophie Ayrault^a

^a Laboratoire des Sciences du Climat et de l'Environnement (LSCE/IPSL), Unité Mixte de Recherche 8212 (CEA, CNRS, UVSQ), 91198, Gif-sur-Yvette Cedex, France

^b Center for Research in Isotopes and Environmental Dynamics (CRIED), University of Tsukuba, 1-1-1 Tennodai, Tsukuba, Ibaraki 305-8572, Japan

* Corresponding author.

E-mail address: hugo.lepage@lsce.ipsl.fr (H. Lepage).

Telephone: +33/1/69.82.43.33

List of authors

Hugo LEPAGE

Laboratoire des Sciences du Climat et de l'Environnement

F-91198 Gif-sur-Yvette Cedex

France

E-mail : hugo.lepage@lsce.ipsl.fr

Tel : +33/1/69 82 43 33

Olivier Evrard

Laboratoire des Sciences du Climat et de l'Environnement

F-91198 Gif-sur-Yvette Cedex

France

E-mail : olivier.evrard@lsce.ipsl.fr

Tel : +33/1/69 82 35 20

Yuichi Onda

Graduate School of Life and Environmental Sciences,

University of Tsukuba,

1-1-1 Tennodai, Tsukuba, Ibaraki 305-8572, Japan

E-mail : onda@geoenv.tsukuba.ac.jp

Tel : +81-29-853-4226

Irène Lefèvre

Laboratoire des Sciences du Climat et de l'Environnement

F-91198 Gif-sur-Yvette Cedex

France

E-mail : irene.lefevre@lsce.ipsl.fr

Tel : +33/1/69 82 43 65

J. Patrick Lacey

Laboratoire des Sciences du Climat et de l'Environnement

F-91198 Gif-sur-Yvette Cedex

France

E-mail : placeby@lsce.ipsl.fr

Sophie Ayrault

Laboratoire des Sciences du Climat et de l'Environnement

F-91198 Gif-sur-Yvette Cedex

France

E-mail : sophie.ayrault@lsce.ipsl.fr

Tel : +33/1/69 82 43 54

Highlights

- Depth migration of ^{137}Cs were investigated in soil cores collected on contaminated paddy field.
- Major part of ^{137}Cs remain in the uppermost 5 cm even 30 months after the accident.
- More than 50% of contamination could remain in tilled soil after decontamination.
- Radiocesium migrate in the uppermost 3 cm after grass cutting.

1 Depth distribution of cesium-137 in paddy fields across the 2 Fukushima pollution plume in 2013

4 Abstract

5 Large quantities of radiocesium were deposited across a 3000 km² area northwest of the
6 Fukushima Dai-ichi nuclear power plant after the March 2011 accident. Although many studies
7 have investigated the fate of ¹³⁷Cs in soil in the months following the accident, the depth
8 distribution of this radioactive contaminant in rice paddy fields requires further examination
9 after the typhoons that occurred in this region. Such investigations will help minimize potential
10 human exposure in rice paddy fields. Radionuclide activity concentrations, organic content and
11 particle size were analysed in 10 soil cores sampled from paddy fields in November 2013, 20
12 km north of the Fukushima power plant. Our results demonstrate limited depth migration of
13 ¹³⁷Cs with the majority concentrated in the uppermost layers of soils (<5 cm). More than 30
14 months after the accident, between 46.8 to 98.7% of the total ¹³⁷Cs inventories was found within
15 the top 5 cm of the soil surface, despite cumulative rainfall totalling 3300 mm. Furthermore,
16 there were no significant correlations between ¹³⁷Cs depth distribution and the other parameters.
17 We attributed the maximum depth penetration of ¹³⁷Cs to grass cutting (73.6-98.5% of ¹³⁷Cs in
18 the upper 5 cm) and farming operations (tillage – 46.8-51.6% of ¹³⁷Cs in the upper 5 cm). As
19 this area is exposed to erosive events, ongoing decontamination works may increase soil
20 erodibility. We therefore recommend the rapid removal of the uppermost – contaminated –
21 layer of the soil after removing the vegetation to avoid erosion of contaminated material during
22 the subsequent rainfall events. Further analysis is required to thoroughly understand the impacts
23 of erosion on the redistribution of radiocesium throughout the Fukushima Prefecture.

24

25 1 Introduction

26 The Tohoku earthquake and the subsequent tsunami on March 11, 2011 resulted in the
27 Fukushima Dai-Ichi Nuclear Power Plant (FDNPP) accident and the significant corresponding
28 atmospheric release of radionuclides, such as ¹³⁷Cs (T_{1/2} = 30 years) (Saunier et al., 2013).
29 Approximately 80% of the release was transported over the Pacific Ocean with the remainder
30 predominantly deposited on Fukushima Prefecture soils as a result of wet atmospheric fallout

31 (Kawamura et al., 2011). Estimations of ^{137}Cs total activity in the Fukushima Prefecture soils
32 range between 10 PBq and 50 PBq, with deposition characterized by strong spatial
33 heterogeneities (Koo et al., 2014). The highest activities are concentrated within a 70 km long
34 radioactive plume where initial ^{137}Cs contamination exceeded $300 \text{ kBq}\cdot\text{m}^{-2}$ covering an area of
35 3000 km^2 . Therefore it is crucial to understand and monitor the fate of the initial radioactive
36 deposits in order to protect the local population against exposure to high dose rates due to
37 gamma radiation that may prevail in areas accumulating contamination.

38 In the coastal catchments affected by the FDNPP accident, Chartin et al. (2013) showed that
39 paddy fields are one of the major sources of ^{137}Cs mobilization and export by soil erosion. A
40 significant proportion of paddy fields are located in the upstream area of the contaminated
41 catchments and they were shown to supply large quantities of contaminated sediment to rivers
42 during typhoons and snowmelt events (Evrard et al., 2013; Evrard et al., 2014). Dispersion of
43 contamination originating from paddy fields along the rivers of the region could therefore
44 contaminate downstream areas that were affected to a limited extent by the initial fallout. In
45 this region, background levels of ^{137}Cs from fallout from atmospheric nuclear weapons testing
46 were estimated to be under $100 \text{ Bq}\cdot\text{kg}^{-1}$ (Fukuyama et al., 2005). Several studies have shown that
47 ^{137}Cs has a low mobility in most soils (Beck 1966, Ivanov et al., 1997) and is rapidly fixed to
48 fine particles, especially clay minerals (Sawhney, 1972; He & Walling, 1996). These findings
49 were confirmed in the vicinity of the main contamination plume in the Fukushima Prefecture
50 where Saito et al. (2014) reported that ^{137}Cs was concentrated in the silt and clay fractions.
51 Also, it was reported that the majority of ^{137}Cs remained in the first centimetre of the soil profile
52 (Fujiwara et al., 2012; Kato et al., 2012; Koarashi et al., 2012; Lepage et al., 2014). However,
53 it was also shown that in soils with high levels of organic matter, radiocesium may migrate
54 down the soil profile as organic matter may reduce its affinity with clay minerals (Kamei-
55 Ishikawa et al., 2008; Koarashi et al., 2012; Staunton et al., 2002; Szenknect et al., 2003).
56 Koarashi et al. (2012) analysed several soil profiles sampled in the vicinity of Fukushima City
57 and showed that clay content and Total Organic Carbon (TOC) were the main factors
58 controlling radiocesium depth migration. They also found a strong negative correlation ($r = -$
59 0.79 , $p < 0.005$) between TOC content divided by clay content (TOC/Clay) and the percentage
60 of retention of ^{137}Cs suggesting that the presence of organic matter inhibits the adsorption of
61 ^{137}Cs on clay minerals.

62 Thirty months after the accident, it is important to investigate the depth distribution of ^{137}Cs in
63 a selection of paddy fields located within the main contamination plume of Fukushima
64 Prefecture. The concentration of ^{137}Cs in the uppermost layers of the soil could make it available
65 for erosion and delivery to nearby rivers. This investigation of ^{137}Cs depth distribution in paddy
66 fields is particularly timely in the current post-accidental phase characterised by the
67 implementation of large-scale remediation efforts targeting paddy fields. The implications of
68 these findings for potential soil erosion will be specifically discussed.

69 **2 Materials and methods**

70 **2.1 Study area**

71 The study was conducted in Fukushima Prefecture, located in North-Eastern Japan, 30 km
72 northwest of FDNPP (Fig. 1). We focused our work on two coastal catchments (i.e. Mano and
73 Niida River catchments - 450km²) draining the main part of the radioactive plume. These
74 catchments extend from the coastal mountain range (approximately 30 km from the coast) to
75 the Pacific Ocean, and their elevation ranges from 0 to 900 m. Mean annual rainfall was 1320
76 mm according to Japanese Meteorological Agency (2014) measured over 37 years at the rainfall
77 station located in the upper part of the Nitta catchment (Fig. 1). Our study was conducted in
78 November 2013 and cumulative rainfall reached 3300mm (max = 35mm.h⁻¹) between the
79 accident and our field survey (32 months) with the occurrence of 4 typhoons (Songda and Roke
80 in 2011, Man-Yi and Wipha in 2013). In these catchments, paddy fields are predominantly
81 located along the rivers (Tanaka et al., 2013).

82 Remediation works implemented since July 2012 under the supervision of the Japanese
83 Ministry Of Environment, Government of Japan (MOE, 2012a; MOE, 2013) are concentrated
84 in upper parts of the Nitta River catchment and consist of removing the five uppermost
85 centimetres of the soil (Mizoguchi, 2013; Sakai et al., 2014) to decrease the radioactive dose
86 level in order to avoid exceeding the permissible level (1 mSv y⁻¹) determined by Japanese
87 authorities (MOE, 2012b).

88 **2.2 Sample collection and preparation**

89 A radiameter (LB123 D-H10, Berthold Technologies) was used to measure radiation dose rates
90 at the ground level in the paddy fields (Table 1). To be representative, dose levels were
91 measured at 5 different locations on each field within 10m². The formula Eq. (1) proposed by

92 the Ministry of Environment MOE (2012b) was then applied to convert these data into annual
93 dose rates.

$$94 \quad D_{an} = \frac{(D_{amb} - 0.04) * (8 + 16 * 0.4) * 365}{1000} \quad (1)$$

95 Where D_{amb} is the ambient dose rate, and D_{an} is the annual dose rates.

96 Soil cores (Table 1) were collected in paddy fields across the two selected catchments (Fig 1).
97 We selected the fields to cover a range of dose rates (low, medium and high) in order to
98 investigate migration of ^{137}Cs in fields with different levels of contamination (Table 1).

99 A soil auger (diameter 45 mm) was used to sample soil cores to a depth of 10 cm from 10 fields.
100 The soil cores were sub-sectioned into 1 cm increments for the uppermost 5 cm (0-1; 1-2; 2-3;
101 3-4; 4-5 cm) and an additional 5 cm increment was taken from 5 cm to 10 cm (5-10 cm).
102 Because of the very high radioactive dose rate measured at the location where core P9 was
103 sampled ($5.5 \mu\text{sv}\cdot\text{h}^{-1}$), two additional layers were sampled at greater depths (10-15 cm and 15-
104 20 cm). Density of the soil was determined by dividing the dry soil mass in each layer by its
105 volume determined from the diameter of the soil auger and the thickness of the layer. Mean
106 compaction in the cores was estimated to be 13% using soil density. Soil TOC content was
107 measured with the dry combustion method (VarioTOC, Elementar, LAME, IRSN, Fontenay
108 aux Roses, France) and clay content (particle size $< 10\mu\text{m}$) of the samples was measured using
109 a laser diffraction system (Malvern Mastersizer 2000) coupled to a liquid dispersing unit (Hydro
110 2000G, University of Paris Sud, Orsay, France). XRD measurement were performed on a
111 diffractometer (INEL XRG 3000, L3MR, CEA, Saclay, France) equipped with a curved
112 position sensitive detector CPS 120 and radiation were produced at 30 kV and 30 mA.

113 **2.3 Gamma spectrometry measurements**

114 Before measurement, samples were dried in an oven at 40°C for a week, ground to a fine powder
115 in an agate mortar, and then packed into 15 mL polyethylene specimen containers. Cesium-137
116 activities were determined by gamma spectrometry using low-background coaxial N- and P-
117 types HPGe detectors (Canberra/Ortec). Counting times of samples varied between 80 000 s
118 and 150 000 s. The ^{137}Cs activities were measured at the 661 keV emission peak. Counting
119 efficiencies and energy calibration were monitored using internal, national (IRSN) and certified
120 International Atomic Energy Agency (IAEA) reference materials (i.e., IAEA-135, IAEA-375,
121 IAEA-CU-2006-03, IAEA-Soil-6, RGU-1, and RGTh-1) prepared in the same specimen

122 containers as the samples. Uncertainties were estimated by combining counting statistics and
123 calibration uncertainties. Summing and self-absorption effects were taken into account by
124 measuring reference materials with similar densities and characteristics as the collected
125 samples. All activities were decay corrected to the date of 14 March 2011 corresponding to the
126 date of the main radionuclide deposits on soils (Kinoshita et al., 2011; Shozugawa et al., 2012).

127 **2.4 Distribution of ¹³⁷Cs with depth**

128 Radiocesium profiles in undisturbed soils are expected to display an exponential decline with
129 depth (He & Walling, 1997; Walling & He, 1999), which can be described by the following
130 function (Beck, 1966):

$$131 \quad C(x) = C_0 * \exp^{-\alpha \cdot x} \quad (2)$$

132 Where $C(x)$ is the concentration activity of a radionuclide in Bq.kg^{-1} at the depth x (cm) and C_0
133 at $x=0$, and α (cm^{-1}) is a coefficient representing the characteristics of the radionuclide
134 distribution and depends on different characteristics of the soil (e.g. pH, CEC, TOC, clay
135 content).

136 In addition, a more specific model can be used to describe ¹³⁷Cs mobility in soils (Kato et
137 al., 2012; Koarashi et al., 2012; Miller et al., 1990):

$$138 \quad I_{(x)} = I_t (1 - \exp^{-z/h_0}) \quad (3)$$

139 Where $I_{(z)}$ is the ¹³⁷Cs inventory (Bq.m^{-2}) at the z (kg.m^{-2}) depth, I_t is the total ¹³⁷Cs inventory
140 and h_0 is the relaxation mass depth (kg.m^2), an index characterising the ¹³⁷Cs penetration in the
141 soil. The greater the value of the relaxation mass depth h_0 , the deeper the ¹³⁷Cs penetrates into
142 the soil profile (Kato et al., 2012).

143 In order to use this formula, we calculated the ¹³⁷Cs inventory using ¹³⁷Cs activities (Bq.kg^{-1})
144 (Lee et al., 2013) at the successive (x) depths (Eq. 4):

$$145 \quad I(x) = \rho(x) * h(x) * A(x) \quad (4)$$

146 Where ρ is the dry bulk density (g.m^{-3}), h is the thickness (cm) of the layer and A the activity
147 (Bq.kg^{-1}) of this layer.

148 **3 Results and discussion**

149 **3.1 Depth distribution**

150 Based on the distribution of ^{137}Cs activity with depth, soil cores were classified into four groups
151 (undisturbed, decontaminated, tilled and managed) (Table 2 - Fig 2) :

- 152 • Undisturbed: distribution shown an exponential decrease of ^{137}Cs activity with depth (Fig
153 3),
- 154 • Decontaminated: very low level of ^{137}Cs activity in all layers,
- 155 • Tilled: similar level of ^{137}Cs activity in each layer,
- 156 • Managed: similar level of contamination in the upper 2-3cm then exponential decrease
157 with depth of the ^{137}Cs activity.

158 The group of undisturbed fields (P6, P7 and P9) remained abandoned by the end of 2013 as
159 they were protected by a dense grass cover (Fig 4a) and they showed an exponential decrease
160 of ^{137}Cs activities with depth (Fig 3). Furthermore, our results on relaxation mass depths h_0 in
161 undisturbed soils (Table 2) varied from 5.4 to 8.3 and remained in the same range as previous
162 results found for soils collected in this area (Table 3). Although this result indicates a limited
163 migration of ^{137}Cs , contamination from the FDNPP accident could still be found at the 10-15
164 cm and 15-20 cm layers in P9 (respectively 370 and 170 $\text{Bq}\cdot\text{kg}^{-1}$, Fig 2). This is likely due to
165 the natural migration of ^{137}Cs as this soil core was heavily contaminated ($155 \text{ kBq}\cdot\text{kg}^{-1}$) and
166 contained 8.5% of TOC. Nevertheless, level of contamination corresponded to less than 10%
167 of total contamination of P9, as observed in the other undisturbed soil cores.

168 The core P5 did not show evidence of additional contamination of ^{137}Cs due to Fukushima
169 accident (Fig 2) as at this site the ^{137}Cs concentration levels remained similar to pre-accident
170 conditions, which were estimated not to exceed $100 \text{ Bq}\cdot\text{kg}^{-1}$ in Japanese soils (Fukuyama et al.,
171 2005). However, the detection of ^{134}Cs confirms that this field was contaminated by the
172 Fukushima fallout and subsequently decontaminated by remediation efforts (Fig 4b -
173 Mizoguchi, 2013; Sakai et al., 2014).

174 P2 and P4 were disturbed after the initial radionuclide deposition, resulting in a homogenization
175 of activities in successive soil layers (Fig 2; Fig 3). These fields were most likely tilled by
176 farmers (Endo et al., 2013; Matsunaga et al., 2013; Yamaguchi et al., 2012) and now around

177 51% of the total contamination inventory is found deeper in the soil (i.e. 5-10 cm) (Table 2).
178 This percentage could be higher ($\approx 66\%$) as tilled soils generally showed a similar level of
179 contamination until 15 cm (Endo et al., 2013; Yamaguchi et al., 2012). Thus, a greater sampling
180 depth should be considered for future investigations on ^{137}Cs migration in Fukushima soils. The
181 ongoing farming operations in this area can be explained by the fact that those fields are not
182 located in the evacuation-prepared area and that cultivation is allowed (Fig 1).

183 In contrast, managed fields (P1, P3, P8 and P10) showed a similar level of contamination in the
184 upper 2-3 centimetres and then a decrease (Fig 2). These four fields have been continuously
185 managed since the accident, as illustrated by our field observations during previous campaigns
186 (Nov. 2011, April 2012 and May 2013). Grass was cut each year using heavy machinery
187 (Fig 4c), which may explain the mixing of soil and associated ^{137}Cs in these fields due to the
188 compaction of the first few centimetres of the soil (Jagercikova et al., 2014; Matsunaga et al.,
189 2013). Takahashi et al. (2014) also reported the same migration in the uppermost 3-centimetres
190 and concluded that it was caused by the repeated formation and melting of needle ice in the
191 surface soil during winter and spring. Further investigation is required to clarify the process
192 involved in this migration. However, our results demonstrated that 73.6 to 98.5% of the ^{137}Cs
193 contamination was concentrated in the upper 5 cm (Table 2).

194

195 Contrary to the results obtained by Koarashi et al. (2012), no significant correlation was found
196 between TOC, clay content, TOC/Clay and both the α coefficient and the relaxation mass depth
197 h_0 (Table 4) in both managed and undisturbed soils (number of samples = 7). As the depth
198 distribution of ^{137}Cs in soils does not vary with the soil parameters, the different ^{137}Cs migration
199 observed between undisturbed and managed fields is most likely explained by the type and
200 frequency of farming operations carried out between the nuclear accident and the sampling
201 campaign. The limited migration of ^{137}Cs could be attributed to the presence of phyllosilicate
202 minerals as identified by XRD analyses (data not presented). These results confirm those found
203 for undisturbed soils located under different land uses in the vicinity of the FDNPP by previous
204 studies (Table 3). Most of these studies concluded that ^{137}Cs was exclusively found in the upper
205 5 cm for undisturbed soil in forests (mean of ^{137}Cs inventory = $94.8 \pm 2.5\%$) and in fields
206 ($98.7 \pm 1.8\%$). Our results on tilled soils are also consistent with those from previous publications
207 (Endo et al., 2013; Koarashi et al., 2012; Matsunaga et al., 2013; Tanaka et al., 2013).

208 To complement the published research conducted a few months after the accident (Fig 5 – Table
209 4), our results showed that even more than 30 months after the accident and after the occurrence
210 of several typhoons (Fig 5), the depth migration of ^{137}Cs was very limited with the majority
211 (73.6 – 98.7%) of this radionuclide still found in the upper 5 centimetres of undisturbed and
212 managed soils. These results are complementary with the study of Mastunaga et al. (2013) who
213 concluded that radiocesium did not migrate with depth even after rainfalls, 5 months after the
214 accident. Tilling is the main contributor of the migration of radiocesium in soil as the main part
215 of contamination is under the first layers (48.4 – 53.2%) in tilled fields (Table 3).

216 **3.2 Implications for contamination redistribution across the catchments**

217 In most of the investigated soil cores, contamination was concentrated in the upper layers of
218 the soils and is therefore potentially available for soil erosion (Motha & Wallbrink, 2002;
219 Walling & Woodward, 1992). However, in abandoned fields, the dense grass cover will protect
220 the soil against erosion as soil erodibility is mainly controlled by the vegetation cover, surface
221 roughness and crusting characteristics (Evrard et al., 2008; Le Bissonnais et al., 2005). During
222 decontamination operations, the grass is cut and vegetation is removed leaving the soil bare and
223 exposed to the erosive impact of intense rainfall. The specific supply of contaminated sediment
224 from fields where remediation efforts were concentrated to nearby rivers was demonstrated by
225 Evrard et al (2014) who showed an increase of radioactive dose rates in recent sediment drape
226 deposits collected in upper parts of the Nitta River catchment after the heavy typhoons that
227 occurred during summer in 2013.

228 In this context, we recommend rapidly removing the first few centimetres of the soil
229 immediately after removing the vegetation to avoid erosion of contaminated material during
230 the subsequent rainfall events. Alternatively, remediation efforts could be concentrated before
231 July or after October, when typhoons are unlikely to occur. We do not recommend mixing soil
232 with water (puddling) in contaminated fields, as this could export the contamination contained
233 in the uppermost layers of the soil (Wakahara et al., 2013). Furthermore, contaminated soils
234 that have been eroded and transported by the river could be deposited on top of already
235 decontaminated soil (Sakai et al. 2014). To avoid this recontamination, we recommend to start
236 the decontamination works in the catchment headwaters and to proceed downstream.

237 **4 Concluding remarks**

238 Depth distributions of ^{137}Cs investigated in 10 paddy fields varied with land management. The
239 maximum depth penetration of ^{137}Cs collected in November 2013 was attributed to maintenance
240 and farming operations in paddy fields contaminated after the FDNPP accident (March 2011).
241 In tilled fields, the contamination showed a similar level in each layer (0-10cm) while in
242 managed field, where vegetation was removed, contamination only migrated down the first
243 2-3 cm. In undisturbed soils, ^{137}Cs inventory decreased with depth following an exponential
244 function. Our results confirm the overall limited migration of ^{137}Cs concentrated in the first few
245 centimetres (<5 cm) of soil in undisturbed and managed paddy fields located within the main
246 Fukushima contamination plume.

247

248 **Author contribution**

249 H.L. and O.E. wrote the main manuscript; O.E. and Y.O. designed research; H.L. and O.E.
250 conducted field sampling; H.L. and I.L. conducted laboratory measurements. Y.O., J.P. L. and
251 S.A. participated to the redaction and reviewed the manuscript.

252

253 **Acknowledgements**

254 This work has been supported by ANR (*French National Research Agency*) and JST (*Japan*
255 *Science and Technology agency*) in the framework of the joint TOFU ANR Flash/J-RAPID
256 Franco-Japanese project (ANR-11-JAPN-001). This work has also been supported by CNRS in
257 the framework of the NEEDS-Environnement HAMUSUTA project, and by the Institute of
258 Environmental Radioactivity (IER) in Fukushima University. Finally, funding from ANR in the
259 framework of the AMORAD project (ANR-11-RSNR-0002) is gratefully acknowledged. Hugo
260 Lepage received a PhD fellowship from CEA (Commissariat à l'Energie Atomique et aux
261 Energies Alternatives, France). The authors would like to thank A. Ritt for conducting TOC
262 measurement and C. Latrille for XRD measurement.

263

264 **References**

- 265 Beck, H.L., 1966. Environmental gamma radiation from deposited fission products. *Health*
266 *Phys.* 12, 313.
- 267 Chartin, C., Evrard, O., Onda, Y., Patin, J., Lefèvre, I., Ottlé, C., Ayrault, S., Lepage, H., Bonté,
268 P., 2013. Tracking the early dispersion of contaminated sediment along rivers draining the
269 Fukushima radioactive pollution plume. *Anthropocene* 1, 23–34.
- 270 Endo, S., Kajimoto, T., Shizuma, K., 2013. Paddy-field contamination with ¹³⁴Cs and ¹³⁷Cs
271 due to Fukushima Dai-ichi Nuclear Power Plant accident and soil-to-rice transfer coefficients.
272 *J. Environ. Radioact.* 116, 59–64
- 273 Evrard, O., Vandaele, K., Biellers, C., Van Wesemael, B., 2008. Seasonal evolution of runoff
274 generation on agricultural land in the Belgian loess belt and implications for muddy flood
275 triggering. *Earth Surf. Process. Landforms* 1301, 1285–1301.
- 276 Evrard, O., Chartin, C., Onda, Y., Patin, J., Lepage, H., Lefèvre, I., Ayrault, S., Ottlé, C., Bonté,
277 P., 2013. Evolution of radioactive dose rates in fresh sediment deposits along coastal rivers
278 draining Fukushima contamination plume. *Sci. Rep.* 3, 3079.
- 279 Evrard, O., Chartin, C., Onda, Y., Lepage, H., Cerdan, O., Lefèvre, I., Ayrault, S., 2014.
280 Renewed soil erosion and remobilisation of radioactive sediment in Fukushima coastal rivers
281 after the 2013 typhoons. *Sci. Rep.* 4, 4574.
- 282 Fujiwara, T., Saito, T., Muroya, Y., 2012. Isotopic ratio and vertical distribution of
283 radionuclides in soil affected by the accident of Fukushima Dai-ichi nuclear power plants. *J.*
284 *Environ. Radioact.* 113, 37–44.
- 285 Fukuyama, T., Takenaka, C., Onda, Y., 2005. ¹³⁷Cs loss via soil erosion from a mountainous
286 headwater catchment in central Japan. *Sci. Total Environ.* 350, 238–47.
- 287 He, Q., Walling, D., 1996. Interpreting particle size effects in the adsorption of ¹³⁷Cs and
288 unsupported ²¹⁰Pb by mineral soils and sediments. *J. Environ. Radioact.* 30, 117–137.
- 289 He, Q., Walling, D., 1997. The distribution of fallout ¹³⁷Cs and ²¹⁰Pb in undisturbed and
290 cultivated soils. *Appl. Radiat. Isot.* 48, 677–690.
- 291 Ivanov, Y., Lewyckyj, N., Levchuk, S., 1997. Migration of ¹³⁷Cs and ⁹⁰Sr from Chernobyl
292 fallout in Ukrainian, Belarussian and Russian soils. *J. Environ. Radioact.* 35.

293 Jagercikova, M., Evrard, O., Balesdent, J., Lefèvre, I., Cornu, S., 2014. Modeling the migration
294 of fallout radionuclides to quantify the contemporary transfer of fine particles in Luvisol
295 profiles under different land uses and farming practices. *Soil Tillage Res.* 140, 82–97.

296 Japanese Meteorological Agency:
297 http://www.data.jma.go.jp/obd/stats/etrn/view/annually_a.php?prec_no=36&block_no=1150
298 &year=2013&month=4&day=&view=, last access: 28 July 2014 (in Japanese)

299 Kamei-Ishikawa, N., Uchida, S., Tagami, K., 2008. Distribution coefficients for ⁸⁵Sr and
300 ¹³⁷Cs in Japanese agricultural soils and their correlations with soil properties. *J. Radioanal.*
301 *Nucl. Chem.* 277, 433–439.

302 Kato, H., Onda, Y., Teramaga, M., 2012. Depth distribution of ¹³⁷Cs, ¹³⁴Cs, and ¹³¹I in soil
303 profile after Fukushima Dai-ichi Nuclear Power Plant Accident. *J. Environ. Radioact.* 111, 59–
304 64.

305 Kawamura, H., Kobayashi, T., Furuno, A., In, T., Ishikawa, Y., Nakayama, T., Shima, S.,
306 Awaji, T., 2011. Preliminary numerical experiments on oceanic dispersion of ¹³¹I and ¹³⁷Cs
307 discharged into the ocean because of the Fukushima Daiichi nuclear power plant. *J. Nucl. Sci.*
308 *Technol.* 48, 1349–1356.

309 Kinoshita, N., Sueki, K., Sasa, K., Kitagawa, J., Ikarashi, S., Nishimura, T., Wong, Y.-S., Satou,
310 Y., Handa, K., Takahashi, T., Sato, M., Yamagata, T., 2011. Assessment of individual
311 radionuclide distributions from the Fukushima nuclear accident covering central-east Japan.
312 *Proc. Natl. Acad. Sci. U. S. A.* 108, 19526–9.

313 Koarashi, J., Atarashi-Andoh, M., Matsunaga, T., Sato, T., Nagao, S., Nagai, H., 2012. Factors
314 affecting vertical distribution of Fukushima accident-derived radiocesium in soil under
315 different land-use conditions. *Sci. Total Environ. Environ.* 431, 392–401.

316 Koo, Y.-H., Yang, Y.-S., Song, K.-W., 2014. Radioactivity release from the Fukushima
317 accident and its consequences: A review. *Prog. Nucl. Energy* 74, 61–70.

318 Le Bissonnais, Y., Cerdan, O., Lecomte, V., Benkhadra, H., Souchère, V., Martin, P., 2005.
319 Variability of soil surface characteristics influencing runoff and interrill erosion. *Catena* 62,
320 111–124.

321 Lee, S.H., Oh, J.S., Lee, J.M., Lee, K.B., Park, T.S., Lujaniene, G., Valiulis, D., Sakalys, J.,
322 2013. Distribution characteristics of ^{137}Cs , Pu isotopes and ^{241}Am in soil in Korea. *Appl.*
323 *Radiat. Isot.* 81, 315–20.

324 Lepage, H., Evrard, O., Onda, Y., Patin, J., Chartin, C., Lefèvre, I., Bonté, P., Ayrault, S., 2014.
325 Environmental mobility of ^{110m}Ag : lessons learnt from Fukushima accident (Japan) and
326 potential use for tracking the dispersion of contamination within coastal catchments. *J. Environ.*
327 *Radioact.* 130, 44–55.

328 Matsunaga, T., Koarashi, J., Atarashi-Andoh, M., Nagao, S., Sato, T., Nagai, H., 2013.
329 Comparison of the vertical distributions of Fukushima nuclear accident radiocesium in soil
330 before and after the first rainy season, with physicochemical and mineralogical interpretations.
331 *Sci. Total Environ.* 447, 301–14.

332 Ministry of Economy, Trade and Industry (METI), 2014. Areas to which evacuation orders
333 have been issued (April 1, 2014),
334 <http://www.meti.go.jp/english/earthquake/nuclear/roadmap/pdf/140401MapOfAreas.pdf>

335 Ministry of Education, Culture, Sports, Science and Technology (MEXT), 2012. MEXT, Japan
336 http://radioactivity.nsr.go.jp/ja/contents/7000/6289/24/203_0928.pdf (In Japanese)

337 Miller, K.M., Kuiper, J.L., Heifer, I.K., 1990. ^{137}Cs Fallout Depth Distributions in Forest
338 Versus Field Sites: Implications for External Gamma Dose Rates. *J. Environ. Radioact.* 12, 23–
339 47.

340 Mizoguchi, M., 2013. Remediation of Paddy Soil Contaminated by Radiocesium in Iitate
341 Village in Fukushima Prefecture. *Agric. Implic. Fukushima Nucl.* 131–142.

342 Ministry of the Environment, Government of Japan (MOE), 2012a, <http://josen.env.go.jp/en/>
343 Ministry of the Environment, Government of Japan (MOE), 2012b,
344 http://josen.env.go.jp/os/en/osen_05.html (In Japanese)

345 Ministry of the Environment, Government of Japan (MOE), 2013. Progress on Off-site Cleanup
346 efforts in Japan. http://josen.env.go.jp/en/documents/pdf/workshop_july_17-18_2013_01.pdf

347 Motha, J., Wallbrink, P., 2002. Tracer properties of eroded sediment and source material.
348 *Hydrol. Process.* 16, 1983–2000.

349

350 National Institute for Agro-Environmental Sciences (NIAES), 1996. Classification of cultivated
351 soils in Japan: third approximation, Classification Committee of Cultivated Soils.

352 National Institute for Agro-Environmental Sciences (NIAES), digital cropland soil map of the
353 Fukushima prefecture. http://agrimesh.dc.affrc.go.jp/soil_db/map_select_figure.phtml (Last
354 access 05/01/2015 - In Japanese)

355 Saito, T., Makino, H., Tanaka, S., 2014. Geochemical and grain-size distribution of radioactive
356 and stable cesium in Fukushima soils: implications for their long-term behavior. *J. Environ.*
357 *Radioact.* 138C, 11–18.

358 Sakai, M., Gomi, T., Nunokawa, M., Wakahara, T., Onda, Y., 2014. Soil removal as a
359 decontamination practice and radiocesium accumulation in tadpoles in rice paddies at
360 Fukushima. *Environ. Pollut.* 187, 112–5.

361 Saunier, O., Mathieu, a., Didier, D., Tombette, M., Quélo, D., Winiarek, V., Bocquet, M., 2013.
362 An inverse modeling method to assess the source term of the Fukushima Nuclear Power Plant
363 accident using gamma dose rate observations. *Atmos. Chem. Phys.* 13, 11403–11421.

364 Sawhney, B., 1972. Selective sorption and fixation of cations by clay minerals: a review. *Clays*
365 *and Clay Minerals.* 20, 93–100.

366 Shozugawa, K., Nogawa, N., Matsuo, M., 2012. Deposition of fission and activation products
367 after the Fukushima Dai-ichi nuclear power plant accident. *Environ. Pollut.* 163, 243–7.

368 Staunton, S., Dumat, C., Zsolnay, a, 2002. Possible role of organic matter in radiocaesium
369 adsorption in soils. *J. Environ. Radioact.* 58, 163–73.

370 Szenknect, S., Gaudet, J.P., Dewiere, L., 2003. Evaluation of distribution coefficients for the
371 prediction of strontium and cesium migration in a natural sand at different water contents. *J.*
372 *Phys.* IV 107, 1279–1282.

373 Takahashi, J., Tamura, K., Suda, T., 2014. Vertical distribution and temporal changes of ¹³⁷
374 Cs in soil profiles under various land uses after the Fukushima Dai-ichi Nuclear Power Plant
375 accident. *J. Environ. Radioact.* 1-11

376 Tanaka, K., Takahashi, Y., Sakaguchi, A., 2012. Vertical profiles of iodine-131 and cesium-
377 ¹³⁷ in soils in Fukushima prefecture related to the Fukushima Daiichi Nuclear Power Station
378 accident. *Geochem. J.* 46, 73–76.

379 Tanaka, K., Iwatani, H., Takahashi, Y., Sakaguchi, A., Yoshimura, K., Onda, Y., 2013.
380 Investigation of spatial distribution of radiocesium in a paddy field as a potential sink. PLoS
381 One 8, e80794.

382 Teramage, M.T., Onda, Y., Patin, J., Kato, H., Gomi, T., Nam, S., 2014. Vertical distribution
383 of radiocesium in coniferous forest soil after the Fukushima nuclear power plant accident. J.
384 Environ. Radioact. 137, 37–45.

385 Wakahara, T., Onda, Y., Kato, H., 2013. Estimation of radionuclide discharge from paddy fields
386 in two experimental plots with different initial scrapings after the Fukushima Dai-ichi Nuclear
387 Power Plant accident 1–3.

388 Walling, D.E., He, Q., 1999. Improved models for estimating soil erosion rates from cesium-
389 137 measurements. J. Environ. Qual. 28, 611–622.

390 Walling, D.E., Woodward, J.C., 1992. Use of radiometric fingerprints to derive information on
391 suspended sediment sources. Eros. Sediment Transp. Monit. Program. River Basin 210, 153–
392 164.

393 Yamaguchi, N., Eguchi, S., Fujiwara, H., Hayashi, K., Tsukada, H., 2012. Radiocesium and
394 radioiodine in soil particles agitated by agricultural practices: field observation after the
395 Fukushima nuclear accident. Sci. Total Environ. 425, 128–34.

Figure captions

Figure 1. Map of the study area with location of the soil cores collected within Mano and Nitta River catchments including ^{137}Cs soil inventory decay corrected to the date of 14 June 2011 based on the Japanese Ministry of Education, Culture, Sports, Science and Technology data (MEXT, 2012) and April 2014 restricted access areas delineated by Ministry of Economy, Trade and Industry (METI, 2014).

Figure 2. Depth distribution of ^{137}Cs activity in soil cores. Data on the 4-5 cm layer for P6 were not available (n/a).

Figure 3. Depth distribution of ^{137}Cs inventory in the different groups of contaminated soil cores.

Figure 4. Pictures taken during the sampling campaign (November 2013) and illustrating the difference of land management practices in the field, a) P9 - dense cover of grass on the field showed an absence of land management, b) P5 – land management in the field showed by tractor tracks and c) P8 - grass recently cut and presence of straw residues on the field.

Figure 5. Daily rainfall between FDNPP accident and this sampling campaign. Occurrence of typhoons is indicated on the graph. Timing of sampling campaigns of previous studies dealing with ^{137}Cs migration in soils is also indicated. Takahashi et al. (2014) also sampled at (1) (2) and (3).

Figure 1.

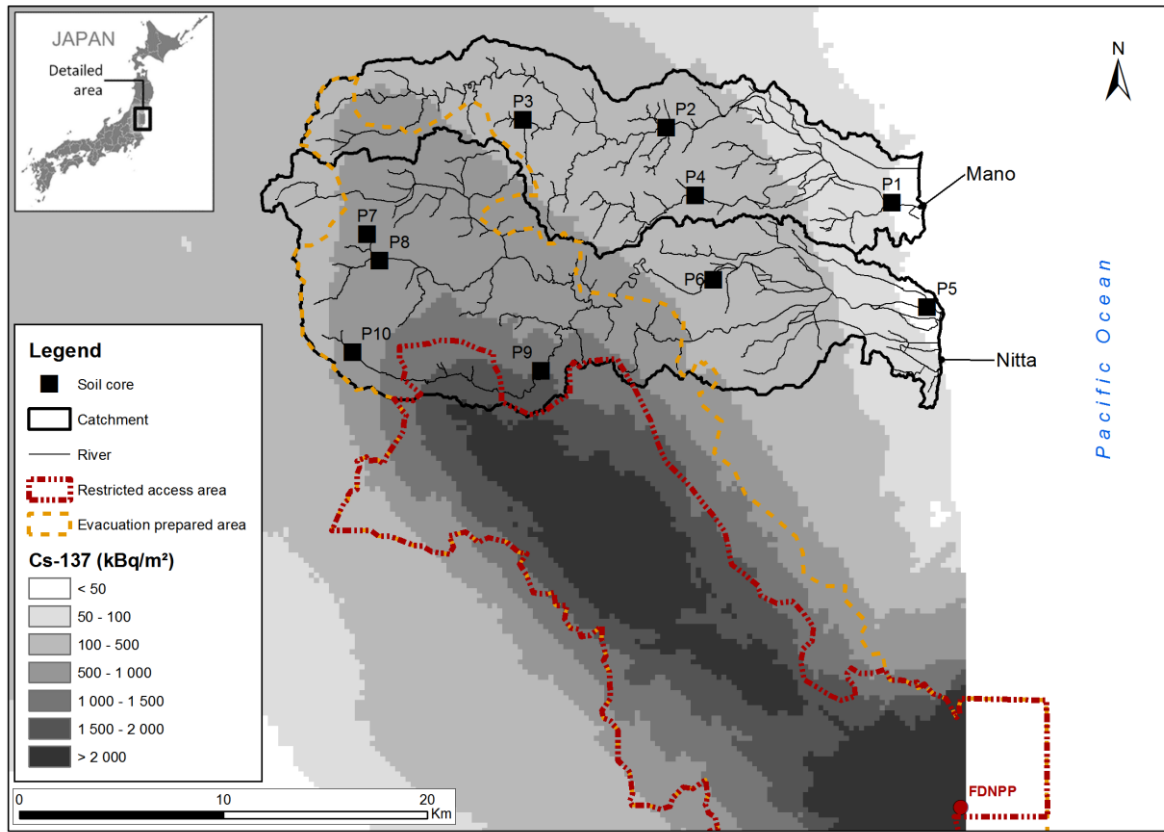


Figure 2

[Click here to download high resolution image](#)

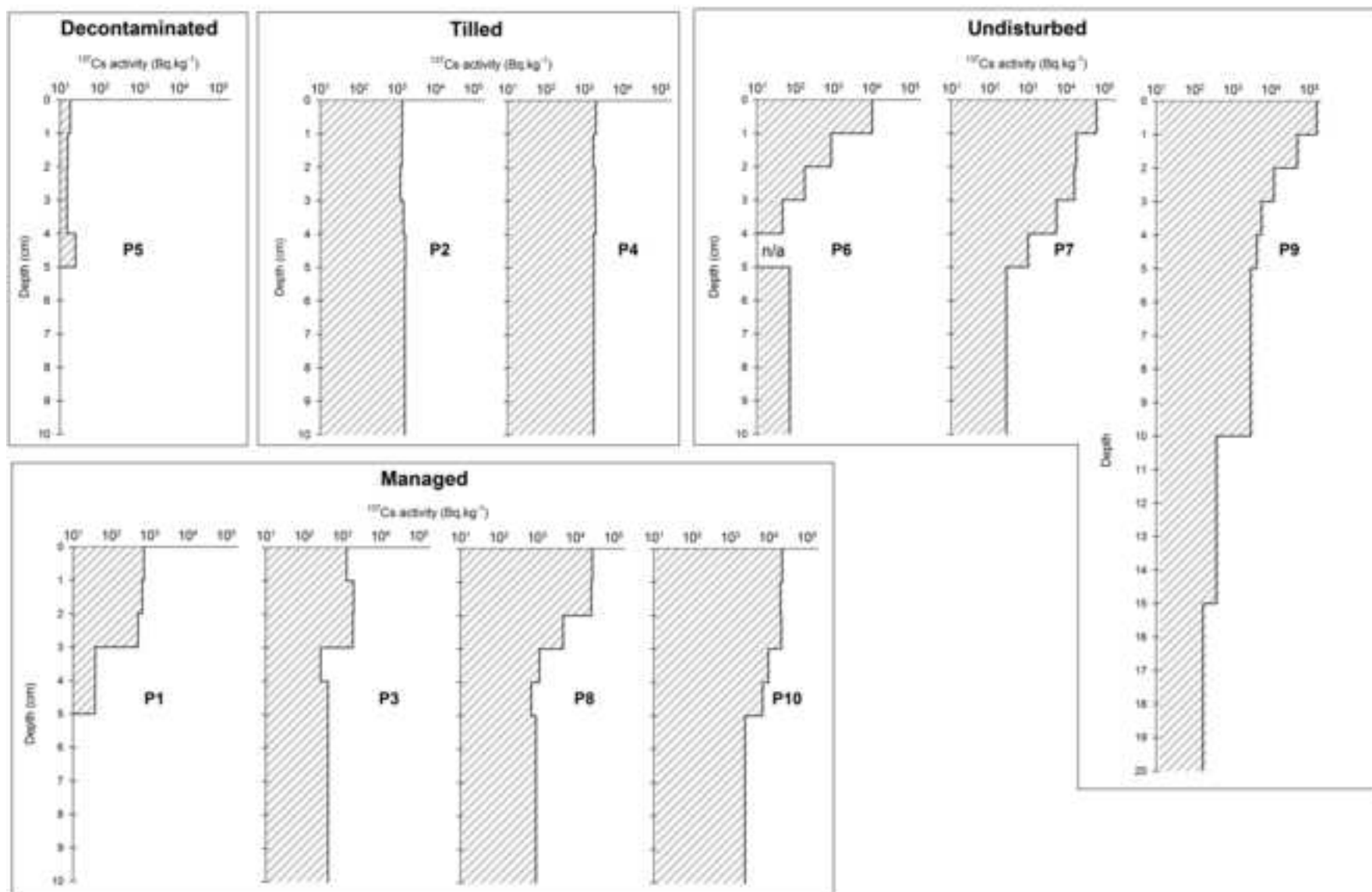


Figure3

[Click here to download high resolution image](#)

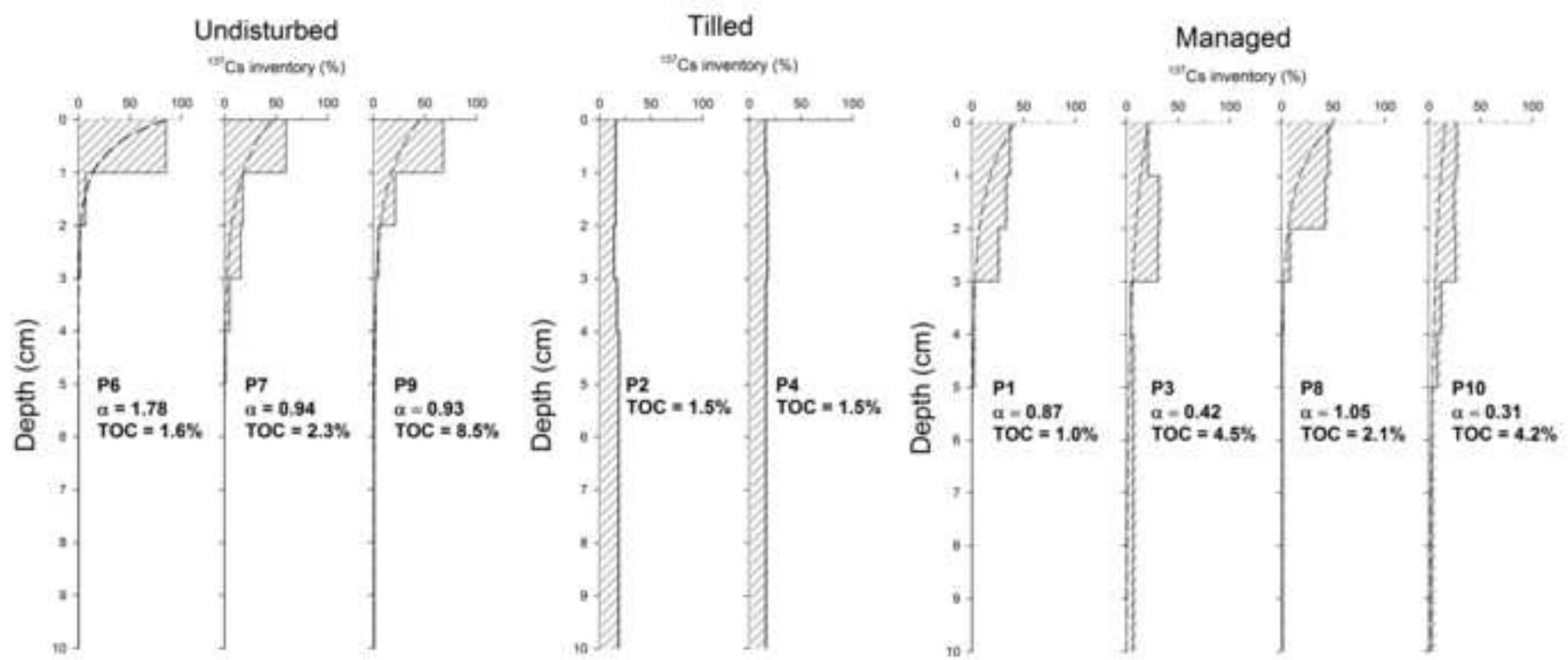


Figure 4.

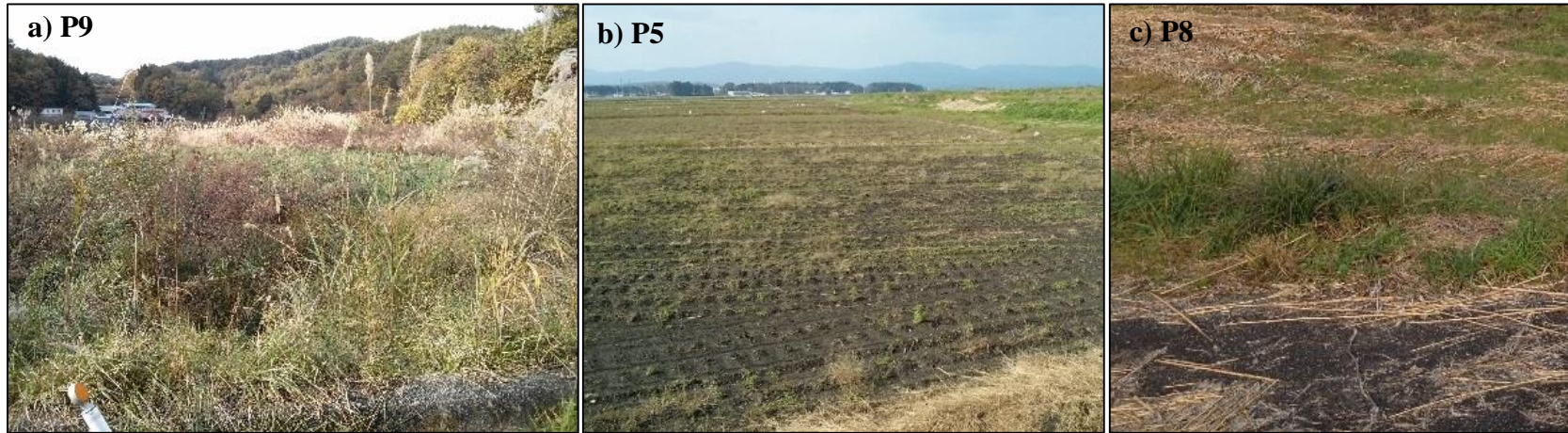


Figure5

[Click here to download Figure: Figure 5.pdf](#)

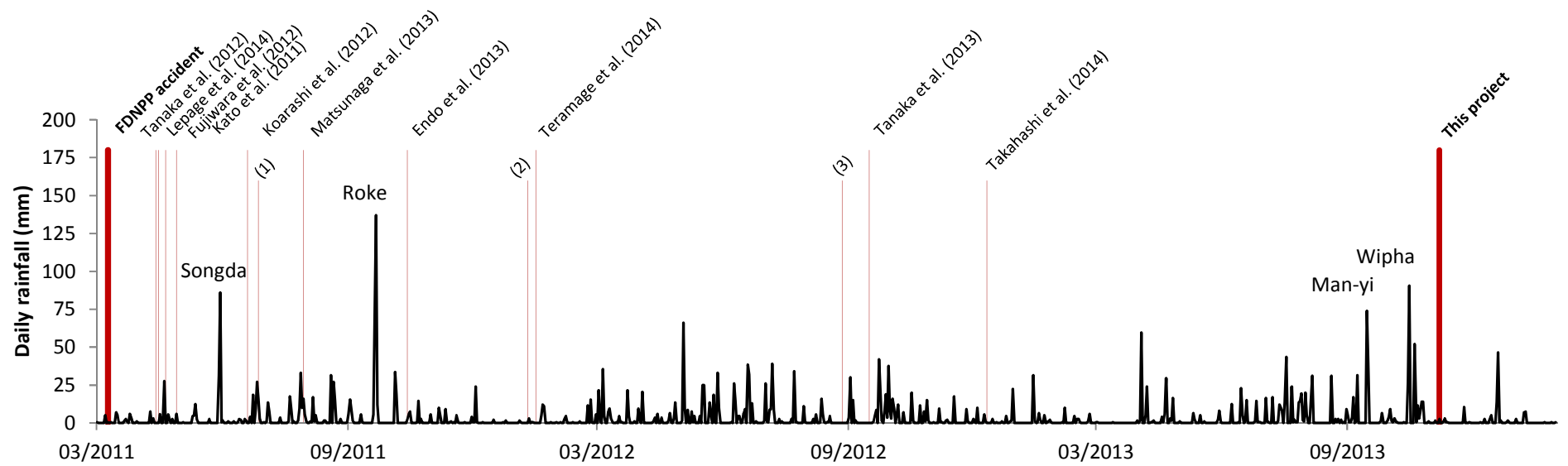


Table1[Click here to download Table: Table 1.docx](#)

Table 1. Location of investigated soil cores and ambient radioactive dose rates measured at the ground level. Annual dose rates exceeding the permissible level of 1mSv.y^{-1} are indicated in bold (MOE, 2012b).

Latitude	Longitude	Profile label	Dose rate ($\mu\text{Sv.h}^{-1}$)	Annual dose rate (mSv.y^{-1})	Japanese soil type (WRB)*
37.688264	140.995708	P1	0.2	0.8	Unknown
37.721432	140.870119	P2	0.4	1.9	Gray lowland soil (Gleyic Fluvisol)
37.724665	140.790469	P3	1.2	6.1	Gray lowland soil (Gleyic Fluvisol)
37.691504	140.886210	P4	0.5	2.4	Gray lowland soil (Gleyic Fluvisol)
37.642013	141.015405	P5	0.1	0.3	Unknown
37.654186	140.896448	P6	1.5	7.7	Gray lowland soil (Gleyic Fluvisol)
37.674029	140.703817	P7	2.7	14.0	Peat soil (Histosol)
37.662245	140.710906	P8	2.3	11.9	Gray lowland soil (Gleyic Fluvisol)
37.613850	140.800832	P9	5.5	28.7	Gray lowland soil (Gleyic Fluvisol)
37.621797	140.695852	P10	2.5	12.9	Gley soil (Gleysol)

* Determined using National Institute for Agro-Environmental Sciences (NIAES) cropland soil map (NIAES, 1996; NIAES)

Table2[Click here to download Table: Table 2.docx](#)

Table 2. Characteristics of the soil cores calculated for the uppermost 5 cm incremental layers. More detail is provided in the Supplementary material

Core	Class	¹³⁷ Cs inventory (%)	Bulk density (g.cm ⁻³)	h0 (kg.m ⁻²)	α (cm ⁻¹)	Mean TOC (%)	Clay (%) d < 10μm
P1	Managed	98.5	1.3 ± 0.3	20.4	0.87	1.0 ± 0.1	14.1 ± 1.1
P2	Tilled	46.8	1.2 ± 0.2	n/a	n/a	1.5 ± 0.2	8.2 ± 0.2
P3	Managed	73.6	0.8 ± 0.2	17.4	0.42	4.5 ± 0.2	10.6 ± 0.9
P4	Tilled	51.6	0.8 ± 0.2	n/a	n/a	1.5 ± 0.1	11.9 ± 2.3
P5	Decontaminated	72.9	1.2 ± 0.2	n/a	n/a	n/a	n/a
P6	Undisturbed	97.1	1.2 ± 0.1	6.3	1.78	1.6 ± 0.3	13.7 ± 2.3
P7	Undisturbed	98.7	0.9 ± 0.2	8.3	0.94	2.3 ± 0.2	10.8 ± 1.1
P8	Managed	92.9	1.1 ± 0.2	10.4	1.05	2.1 ± 0.4	8.3 ± 0.2
P9	Undisturbed	92.8	0.7 ± 0.1	5.4	0.93	8.5 ± 0.3	14.6 ± 1.2
P10	Managed	87.1	0.8 ± 0.1	16.8	0.31	4.2 ± 0.4	16.2 ± 0.6

n/a : not available

Table3

[Click here to download Table: Table 3.docx](#)

Table 4. Literature review of studies investigating evolution of radiocesium activities with depth in soils contaminated by FDNPP radioactive fallout.

Shape	Reference	Sampling period (mm/yy)	Number of samples	Type of land use investigated	Mean of % upper 5 cm	α (cm ⁻¹)	h_0 (kg.m ⁻²)
Disturbed (Tilled)	Endo et al. (2013)	10/11	3	Paddy field	≈50	n/a	n/a
	Koarashi et al. (2012)	06/11	6	Croplands (with one paddy field)	81	n/a	n/a
	Matsunaga et al. (2013)	07/11	6	Croplands (with one paddy field)	80	n/a	n/a
	Tanaka et al. (2013)	09/12	3	Cultivated paddy field	55	n/a	n/a
	This study	11/13	2	Paddy field	49	n/a	n/a
Disturbed (managed, grazing)	Takahashi et al. (2014)	06/11	2	Land	99	0.3	n/a
			3	Field	98	1.0	n/a
		01/12	2	Land	99	0.5	n/a
			3	Field	98	0.6	n/a
		08/12	2	Land	100	0.7	n/a
			3	Field	94	0.5	n/a
		12/12	2	Land	98	0.4	n/a
			3	Field	88	0.6	n/a
This study	11/13	4	Paddy field	88	0.7	18.2	
Undisturbed	Fujiwara et al. (2012)		1	Brown forest soil	n/a	0.7	n/a
			1	Fluvisol	n/a	0.9	n/a
			1	Vegetable field	n/a	2	n/a
	Kato et al. (2011)	04/11	1	Cultivated soil (home garden)	99	1.2	9.1
	Koarashi et al. (2012)		6	Croplands (with one paddy field)	99	1.3	5.3
		06/11	4	Grassland	99	1.2	4.9
			5	Forest	97	0.6	8.4
	Lepage et al. (2014)	04/11	1	Cropland	n/a	1,9	7.1

Matsunaga et al. (2013)	07/11	6	Croplands (with one paddy field)	99	n/a	n/a
		4	Grassland	99	n/a	n/a
		5	Forest	97	n/a	n/a
Takahashi et al. (2014)	06/11	3	Forest	98	0.7	n/a
		2	Land	100	2.0	n/a
	01/12	3	Forest	92	0.6	n/a
		2	Land	100	1.7	n/a
	08/12	3	Forest	96	0.7	n/a
		2	Land	100	1.4	n/a
Tanaka et al. (2012)	04/11	3	Forest	94	0.7	n/a
		2	Land	100	1.3	n/a
		2	Field	95	n/a	n/a
Teramage et al. (2014)	01/12	2	Fruit trees field	92	n/a	n/a
		1	Coniferous forest	92	0.6	11.1
This study	11/13	3	Paddy field	96	1.2	6.7

n/a : not available

Table 4. Correlation coefficients (r) obtained between the vertical distribution parameters and soil properties measured in samples collected in both undisturbed and managed fields

	α	h_0	TOC (%)	Clay (%)	TOC/Clay
α	1				
h_0	-0.66	1			
TOC (%)	-0.35	-0.30	1		
Clay (%)	-0.11	0.13	0.30	1	
TOC/Clay	-0.38	-0.29	0.95*	-0.01	1

* Significant at the 0.01 probability level